Review Article

PET/SPECT molecular imaging in clinical neuroscience: recent advances in the investigation of CNS diseases

Feng-Mei Lu, Zhen Yuan

Bioimaging Core, Faculty of Health Sciences, University of Macau, Taipa, Macau SAR, China

Correspondence to: Zhen Yuan. Bioimaging Core, Faculty of Health Sciences, University of Macau, Taipa, Macau SAR, China. Email: zhenyuan@umac.mo.

Abstract: Molecular imaging is an attractive technology widely used in clinical practice that greatly enhances our understanding of the pathophysiology and treatment in central nervous system (CNS) diseases. It is a novel multidisciplinary technique that can be defined as real-time visualization, *in vivo* characterization and qualification of biological processes at the molecular and cellular level. It involves the imaging modalities and the corresponding imaging agents. Nowadays, molecular imaging in neuroscience has provided tremendous insights into disturbed human brain function. Among all of the molecular imaging modalities, positron emission tomography (PET) and single photon emission computed tomography (SPECT) have occupied a particular position that visualize and measure the physiological processes using high-affinity and high-specificity molecular radioactive tracers as imaging probes in intact living brain. In this review, we will put emphasis on the PET/SPECT applications in Alzheimer's disease (AD) and Parkinson's disease (PD) as major CNS disorders. We will first give an overview of the main classical molecular neuroimaging modalities. Then, the major clinical applications of PET and SPECT along with molecular probes in the fields of psychiatry and neurology will be discussed.

Keywords: Molecular imaging; central nervous system (CNS) diseases; positron emission tomography (PET); single photon emission computed tomography (SPECT)

Submitted Mar 18, 2015. Accepted for publication Mar 23, 2015.
doi: 10.3978/j.issn.2223-4292.2015.03.16
View this article at: http://dx.doi.org/10.3978/j.issn.2223-4292.2015.03.16

Introduction

The human brain is the most complex organ which acts as the center of the nervous system. It is very vulnerable to central nervous system (CNS) diseases such as neurodegenerative disorders including Alzheimer's disease (AD), Parkinson's disease (PD) and multiple sclerosis and also susceptible to psychiatric conditions including schizophrenia and depression. Although the neural mechanisms behind these brain dysfunctions are being studies in neuroscience field, how these cells interact with one another and the detailed molecular or subcellular processes underlying the neurological disorders are yet not well understood (1).

Traditionally, the mechanism of the CNS disorders can be investigated in the late stage or through postmortem analysis. However, the emerging molecular neuroimaging techniques such as magnetic resonance imaging (MRI), X-ray computed tomography (CT), positron emission tomography (PET) and single photon emission computed tomography (SPECT) have made it possible to noninvasively identify the fundamental biological processes of the CNS diseases. In particular, the advantages of molecular imaging lie in that the sophisticated biological processes and specific pathways in a given disease can be elucidated at the cellular and molecular levels in human and other living systems (2). In addition, molecular imaging can provide the information of clinical changes before the pathological features occurred, making it possible to diagnose the diseases at early stage and to help in therapeutic trials of many CNS disorders (3).

Though there are several molecular imaging modalities

available, however, in this review, we will focus on PET/SPECT techniques due to their extensive applications in clinical neurosciences. We begin by a brief introduction of the PET and SPECT together with their strengths and limitations. Then the major applications of the two modalities in the field of CNS disorders such as neurodegenerative disorders (AD and PD) are discussed. Finally we will talk about the future trends in this specific field.

PET/SPECT molecular neuroimaging

PET and SPECT have made a significant contribution for many years as to evaluate the physiological function and biochemical changes of molecular targets. Both techniques are based on the measurement of the radionuclide's decay, during which a positron or a γ-ray will be emitted and thus generate photos. PET and SPECT have many advantages such as high sensitivity, good spatial resolution and limitless penetration depth, leading to their vital role in molecular imaging for both preclinical and clinical studies. In this section, we will first give a brief introduction to the classical molecular neuroimaging modalities. Then, the major clinical applications of PET and SPECT along with their molecular probes in AD and PD will be provided.

Classical modalities for molecular neuroimaging

Table 1 briefly lists some of the general characteristics of representative molecular imaging techniques include CT, MRI, radionuclide imaging, optical imaging and ultrasound imaging. Among those, the optical molecular imaging technologies have not been employed for exploring human brain (4).

Positron emission tomography (PET)

PET records pairs of high energy γ-rays emitted indirectly from the decay of a radioisotope such as ^{11}C, ^{13}N, ^{15}O and ^{18}F which are introduced into the subject. The positrons emitted from radioisotopes travel a few millimeters through the surrounding tissue and then their kinetic energy lose rapidly. Later, they move slowly and interact with electrons to generate two 511 keV γ-rays (known as the annihilation radiation), travelling at nearly opposite directions (5). PET needs to employ the huge and high-cost cyclotron to produce most of the isotopes (6). The radioisotopes must be made at the site and introduced to the subject quickly since they have a short half-life (the time it takes for 50% of the radioactivity to decay) such as ^{18}F: $t_{1/2}$ =109.8 minutes or even ultra-short half-life such as ^{11}C: $t_{1/2}$ =20.3 minutes and ^{15}O: $t_{1/2}$ =2.04 minutes (*Table 2*) (7). In addition, some of isotopes e.g., ^{68}Ga and ^{82}Rb can be generated using a generator. Among all of radioisotopes, the ^{15}O, ^{11}C and ^{18}F are the most extensively used isotopes for brain imaging. Three-dimensional images of functional processes in brain are finally constructed from PET detectors by computer analysis.

PET is a high-performance molecular imaging tool widely used in clinical utility, preclinical arenas and basic research in the field of neurology, cardiology and particular neuro-oncology due to its excellent sensitivity of 10^{-11}-10^{-12} mol/L and limitless depth of penetration. PET scanning with the metabolic tracer [^{18}F]-2-fluoro-2-deoxy-D-glucose ([^{18}F] FDG) is widely used in the clinic oncology for detecting the tumor, staging the cancer and monitoring therapy. [^{18}F] FDG is a glucose analog first synthesized by Ido *et al*. (8) which is transported by glucose-using cells and phosphorylated by hexokinase. It is used extensively as an important biomarker of cancer because the faster metabolism of glucose in cancer cells as compared with normal cells can be measured.

PET can be also used to explore the human brain disorders and diseases. Actually, a normal brain needs to consume large quantity of glucose, however, in a pathological brain of AD, the metabolism of glucose as well as oxygen will significantly decrease. Hence, the [^{18}F] FDG may be an effective marker to successfully identify the AD and to make early diagnosis with frontotemporal dementia.

In addition to its clinical utility, PET can also be applied in preclinical trials to study *in vivo* pharmacology and in small animal models. Nowadays, the miniaturized PET scanner that is small enough has been available for imaging rodents. For example, a Rat Conscious Animal PET (RatCAP) has been constructed which can allow small animal free of anesthesia to be scanned. The specifically designed PET scanner refers to as microPET and has spatial resolution of 1-2 mm and sensitivity of 10^{-11}-10^{-12} mol/L.

Single photon emission computed tomography (SPECT)

SPECT is very similar to PET in its use of radioactive tracer and detection of γ-rays. However, unlike PET the radioisotopes used for SPECT emit only a single γ-ray during decay that is measured directly. Moreover, SPECT scans are significantly less expensive than PET scans partly due to that the nuclides used in SPECT have a longer half-

Table 1 Characteristic of molecular imaging modalities

Modality	Spatial resolution[a]	Temporal resolution[b]	Sensitivity[c]	Advantages	Disadvantages	Physical principle	Depth of penetration	Type of molecular probe	Probe quantity	Ability for human brain imaging
Nuclear CT	50-200 μm	Minutes	10^{-6}	High spatial resolution; excellent penetration depth; fast and cross-sectional images	Low contrast; radiation risk	X-rays	Limitless	May be possible	Not used	Yes
Radionuclide										
PET	1-2 mm	Seconds-Minutes	10^{-11}-10^{-12}	High sensitivity; excellent penetration depth; whole-body imaging	High cost of cyclotron needed; radiation risk	High-energy γ-rays	Limitless	Radiolabeled, directly or indirectly	Nanograms	Yes
SPECT	1-2 mm	Minutes	10^{-10}-10^{-11}	High sensitivity; no tissue penetrating limit; no need for cyclotron	Low spatial resolution; radiation risk; hard to quantify	Low-energy γ-rays	Limitless	Radiolabeled, directly or indirectly	Nanograms	Yes
MRI	25-100 μm	Minutes-Hours	10^{-9}-10^{-6}	High spatial resolution; no tissue penetrating limit; no radiation	Relatively low sensitivity and low contrast; high cost; long scanning time	Radiowaves	Limitless	10^{-9}-10^{-6}	Micrograms-Milligrams	Yes
Optical										
Optical fluorescence imaging	2-3 mm[d]	Seconds-Minutes	10^{-9}-10^{-12}	High sensitivity; no radiation; inexpensive; activatable	Low spatial resolution[e]; attenuation by overlying tissues; poor penetration depth	Visible or near-infrared light	<1 cm[f]	Activatable, directly or indirectly	Micrograms-Milligrams	No
Optical bioluminescence imaging	3-5 mm[d]	Seconds-Minutes	10^{-15}-10^{-17}	High sensitivity; no radiation; inexpensive and simple equipment operation; non-damaging imaging	Low spatial resolution; attenuation by overlying tissues; poor penetration depth	Visible light	1-2 cm	Activatable indirectly[g]	Micrograms-Milligrams	No
Ultrasound	50-500 μm	Seconds-Minutes	Excellent when microbubbles used	No radiation; excellent sensitivity with microbubbles; high temporal resolution; inexpensive	Poor penetration depth; high spatial resolution; low contrast and strong boundary effect	High-frequency sound wave	Millimeters-Centimeters	Limited activatable, directly	Micrograms-Milligrams	Yes

[a], Spatial resolution expresses in millimeters, refers to the minimum distance that the imaging modality can differentiate two independently measured objects; [b], temporal resolution, refers to the duration of time need to acquire enough events to form an image of a dynamic process; [c], sensitivity, refers to the ability to distinguish a molecular probe from the background, the unit is mole per liter; [d], spatial resolution of fluorescence and bioluminescence is depth-dependent. For bioluminescence imaging, the value is equal to or slightly less than the depth of the measured object; [e], with the exception of fluorescence tomography imaging (FTI), which has high spatial resolution capable of imaging at deep depths; [f], this depth refers to reflectance fluorescence. Fluorescence tomography is able to image objects at greater depths of 2-6 cm; [g], bioluminescence may also provide direct imaging using the Renilla luciferase protein. CT, computed tomography; PET, positron emission tomography; SPECT, single photon emission computed tomography; MRI, magnetic resonance imaging.

Table 2 Most common used PET radioisotopes

Radionuclides	^{11}C	^{13}N	^{15}O	^{18}F	^{64}Cu	^{68}Ga	^{82}Rb	^{166}Ho
Energy (keV)	511							
$T_{1/2}$	20.39 m	9.97 m	2.04 m	109.77 m	13 h	67.63 m	1.27 m	27 h

PET, positron emission tomography; m, minutes; h, hours.

Table 3 Most common used SPECT radioisotopes

Radionuclides	^{67}Ga	^{67}Cu	^{99m}Tc	^{111}In	^{123}I	^{153}Sm	^{159}Gd	^{166}Ho	^{177}Lu
Energy (keV)	93	185	140	245	159	103	363	80	208
$T_{1/2}$	3.26 d	3 d	6.06 h	2.83 d	13.2 h	47 h	20 h	26 h	7 d

SPECT, single photon emission computed tomography; d, days; h, hours.

life and are relatively easily obtained than PET.

The γ emitting isotopes for SPECT include ^{99m}Tc ($t_{1/2}$ =6 hours), ^{123}I ($t_{1/2}$ =13.3 hours), and ^{111}In ($t_{1/2}$ =2.8 days) which are heavy radioisotopes and decay via a single photon emission (*Table 3*). SPECT utilize a γ camera to detect γ photons. To acquire SPECT images from numerous positions, the γ camera is rotated around the subject and projections are acquired at defined points during the rotation. The collimator in γ camera is a lead or tungsten which rejects many photos that not propagated along the axis at right angles in order to make sure the origin of emission can be discerned. The disadvantage of this is that collimator absorbs most of the photons, resulting in that the sensitivity of SPECT is several orders of magnitude lower than of PET. Furthermore, the spatial resolution of SPECT is depended on the collimation errors, which are lower than the clinical PET. However, for microSPECT, the spatial resolution can be relatively very high. The microSPECT designed for imaging small animals can be more widely used in preclinical studies such as neurology, oncology and drug development in small animal model. For example, Beekman *et al*. have developed a new rodent SPECT instrument named U-SPECT-I whose spatial resolution can reach at submillimeter in 2005 (9). Amazingly, the same research group has set up a second generation machine called U-SPECT-II whose spatial resolution is less than half a millimeter (10). What's more, the longer half-life radionuclides used in SPECT make it possible to perform longitudinal scans.

It's worth noting that PET cannot be able to distinguish between two different radioisotopes when injected simultaneously owing to isotopes that are positron emitters give rise to two γ-rays with the same energy. SPECT, on the other hand, dose have some multiplexing capabilities because multiple nuclides produce γ-rays with different energies, thus enabling it to image different targets simultaneously (11). For example, Hijnen *et al*. (12) has conducted a dual-isotope experiment using a microSPECT system and has quantified the biodistribution and tumor uptake of the angiogenesis tracer cyclic arginine-glycine-aspartate (cRGD) via SPECT. Recently, Hapdey *et al*. (13) has worked out a generalized spectral factor analysis (GSFA) method for simultaneous ^{99m}Tc/^{123}I SPECT, proving that simultaneous ^{99m}Tc/^{123}I imaging obtained through GSFA can also be of similar quantitative accuracy compared to those using sequential and scatter-free ^{99m}Tc/^{123}I imaging in brain SPECT.

PET/SPECT with molecular imaging agents in CNS diseases

The CNS disorders can arise from trauma, infections, degeneration, structural defects, blood flow disruption, autoimmune disorders, tumors and stroke. There are various types of CNS diseases and conditions, including neurodegenerative diseases such as AD, PD and essential tremor, neurological disorders including attention deficit-hyperactivity disorder (ADHD) and autism, inflammatory demyelinating diseases such as multiple sclerosis and genetic disorders such as Huntington's disease.

It is believed that the molecular imaging approaches have played a promising role in evaluating the physiological mechanisms and pathomechanisms of CNS disorders in living brain of animal models and experimental human models. The molecular imaging agent is of great important during the course of molecular imaging study. The agents

Table 4 Several imaging agents used in PET/SPECT in some CNS disorders

Reference	Imaging agent	PET/SPECT	CNS disorder
Shoghi-Jadid *et al*., 2002 (14)	^{18}F-FDDNP	PET	AD
Brooks *et al*., 1990 (15)	^{18}F-FDOPA	PET	PD
Mintun *et al*., 2006 (16); Klunk *et al*., 2004 (17)	^{11}C-PIB	PET	AD
Farde *et al*., 1990 (18); Hirvonen *et al*., 2008(19)	^{11}C-raclopride	PET	PD, schizophrenia, depression
Banati *et al*., 2000 (20); Groom *et al*., 1995 (21)	^{11}C-PK11195	PET	AD, MS, Huntington's disease
Savic *et al*., 1995 (22)	^{11}C-flumazenil	PET	Epilepsy
Kadir *et al*., 2006 (23)	^{11}C-nicotine	PET	AD
Versijpt *et al*., 2003 (24)	^{123}I-iodo-PK11195	SPECT	AD
Arlicot *et al*., 2008 (25)	^{123}I-CLINDE	SPECT	AD, MS, Huntington's disease
Booij *et al*., 1998 (26)	^{123}I-FP-CIT	SPECT	PD
Winogrodzka *et al*., 2003 (27)	^{123}I-β-CIT	SPECT	PD
Kung *et al*., 1996 (28)	^{99m}Tc-TRODAT	SPECT	PD
Friedland *et al*., 1997 (29)	^{99m}Tc-10H3	SPECT	AD

PET, positron emission tomography; SPECT, single photon emission computed tomography; CNS, central nervous system; AD, Alzheimer's disease; PD, Parkinson's disease; MS, multiple sclerosis.

also can be termed imaging probes, tracers, contrast agent and radiolabeled probes. Ideally, a molecular agent is expected to rapidly bind to or interact with its target and rapidly clear from tissue and have excellent metabolic stability. There are multiple molecular imaging agents including small molecules, peptides, affibodies, aptamers, antibodies and nanoparticles. Among these agents, the small molecules play a significant role in imaging an enormous range of molecular targets especially in CNS targets due to their small size so that they can cross blood brain barrier, enter in the biological system and clear from tissue at a very fast speed. Generally speaking, small molecule imaging agents can be divided into two key types, one is the molecule that is high affinity for ion channels, transporters or specific receptors such as peripheral benzodiazepine receptor (PBR), another is molecular that can be capable reflecting the metabolism or enzymatic activity. In this part, we focus on small molecules and their applications in two major CNS diseases such as AD and PD. *Table 4* lists several examples of small molecules used in PET/SPECT in some CNS disorders.

PET/SPECT molecular imaging in AD

AD, the most common type of dementia which accounts for 60% to 80% of all cases of dementia, is histopathologically characterized by plaques accumulation of abnormally folded beta-amyloid (Aβ) and abnormal aggregation of intra-neuronal neurofibrillary tangles (NFTs) contained hyperphosphorylated tau protein. Recently, the inflammatory mechanism, oxidative stress, lipid dysfunction and neuronal degradation have been supposed to be closely associated with the neurodegenerative process of AD. It is assumed that the excessive accumulation of Aβ in the brain form the insoluble plaques, leading to NFT formation, synaptic dysfunction and neuronal loss. This hypothesis known as the amyloid cascade hypothesis has provided the excellent insight into the molecular mechanisms underlying the AD pathogenesis. Amyloid deposits may serve as an early and inevitable event in AD pathogenesis. *In vivo* imaging of Aβ in AD patients would be therefore of great significance for the early diagnosis and illustration of pathophysiology underlying AD and also the future development of feasible therapy protocols.

In the past decades, several radiological contrast compounds suitable for amyloid imaging have been developed using different strategies, among which the small molecular imaging was so far the most successful one. The specifically binding compounds were developed from radiolabelled Aβ antibodies and peptide fragments (30-32), then small molecules of Congo red, stilbene, thioflavin and acridine for PET and SPECT (33,34) as well as amyloid-binding compounds applicable for MRI are further developed (35,36). However, compounds that are able to provide high

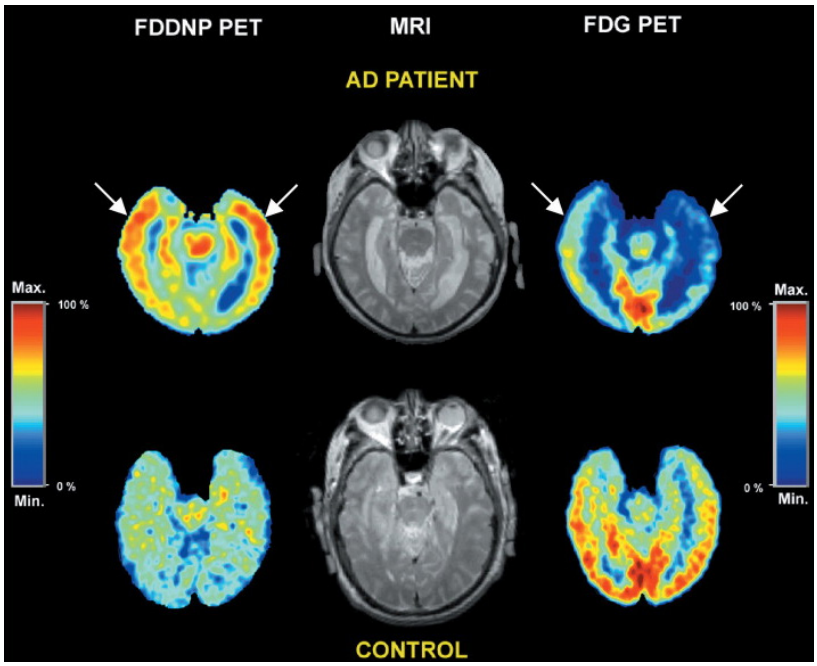

Figure 1 The ^{18}F-FDDNP-PET, MRI, and FDG-PET images for a representative AD patient (the top row) and an HC (the bottom row). The ^{18}F-FDDNP images were acquired by summing frames 12-14, corresponding to 25-54 minutes post-^{18}F-FDDNP injection. The FDG images were obtained by summing frames corresponding to 20-60 minutes post-FDG administration. The arrows display that brain areas with FDG low glucose metabolism are matched with the localization of NFTs and Aps resulting from ^{18}F-FDDNP binding. Reproduced with the permission from ref. (14). PET, positron emission tomography; MRI, magnetic resonance imaging; AD, Alzheimer's disease; HC, healthy control; NFTs, neurofibrillary tangles; Aps, β-amyloid plaques.

selectivity detection for Aβ and tau depositions have not been utilized for clinical study (37-39).

PET imaging of amyloid in AD with ^{18}F-FDDNP

To date, five main radiological compounds including 2-(1-(6-[(2-[^{18}F]fluoroethyl)(methyl)amino]-2-naphthyl) ethylidene)malononitrile (^{18}F-FDDNP), ^{18}F-BAY94-9172, ^{11}C-SB-13, ^{11}C-BF-227 and Pittsburgh Compound-B (^{11}C-PIB) are available as amyloid plaques imaging probes for clinical study. Both the ^{18}F-FDDNP and the ^{11}C-PIB have been routinely adopted by AD patients and the uptakes can be observed in their brains by PET.

^{18}F-FDDNP is a small molecule that binds to both prion plaques and NFTs in human AD brain tissues according to previous investigations on autopsy. Though it remains inconclusive whether ^{18}F-FDDNP possesses high sensitive for the early detection of the underlying pathologies of AD (40), it is the first molecular probe that can non-invasively detect the location of NFTs and Aβ plaques *in vivo*. For example, Shoghi-Jadid and his colleagues used ^{18}F-FDDNP as a molecular imaging probe of PET to exhibit the abnormal amyloid deposition in living AD brain (14). In their study, nine subjects with seven of them are probable AD and others are possible AD together with seven healthy controls (HC) are injected intravenously with ^{18}F-FDDNP. The relative residence time (RRT) in region of interests related to AD is measured and a region with high density of NFT and Aβ plaques is expected with high RRT value. ^{18}F-FDDNP was shown to have a higher RRT in hippocampus, temporal, parietal, occipital and frontal areas in AD than that in healthy subjects. The hippocampus-amygdala-entorhinal regions were reported to have the longest RRT. In *Figure 1*, the ^{18}F-FDDNP-PET, MRI, and FDG-PET images are provided to show the difference between a representative AD patient and a HC.

PET imaging of amyloid in AD with ^{11}C-PIB

The most widely validated amyloid-imaging PET radiotracer compound is N-methyl-[^{11}C]2-(4'-methylaminophenyl)-6-hydroxybenzothiazole termed Pittsburgh Compound-B (PIB). Previous studies have showed that when PIB was intravenous injected in mouse

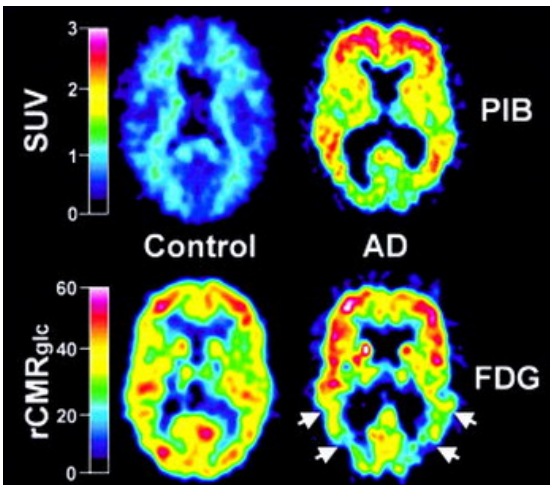

Figure 2 PIB standardized uptake value (SUV) images of PIB retention in a 79-year-old AD patient (right) and a 67-year-old HC (left). PIB and ^{18}FDG images were obtained within 3 days of each other. The SUV PIB images summed over 40-60 minutes are displayed in top and the ^{18}FDG rCMRglc images (μmol/min/100 mL) are shown in bottom. The lack of PIB retention in the entire gray matter and nonspecific PIB retention in the white matter of the HC are showed in the top left column. The normal ^{18}FDG uptake is seen in the bottom left column. The high PIB retention of the AD patient is seen in the frontal and temporoparietal cortices (top right). A typical pattern of ^{18}FDG hypometabolism of AD patient is shown in the temporoparietal cortex (arrows; bottom right) along with preserved metabolic rate in the frontal cortex. Reproduced with the permission from ref. (17). PIB, Pittsburgh Compound-B; AD, Alzheimer's disease; HC, healthy control.

models of AD, the compound was able to enter the brain rapidly and clear rapidly from normal brain tissue (41,42). Recently, Klunk *et al*. (17) utilized ^{11}C-PIB to exhibit the retention of PIB in living brain regions of AD patients. This work involves in 16 patients with mild AD and nine HC. All the subjects were injected about 300 MBq of PIB intravenously and also ^{18}FDG with 200-300 MBq for measurement of the regional cerebral glucose metabolism. Their findings showed that PIB in HC subjects rapidly entered and cleared in brain areas including all cortical and subcortical gray matter as well as cerebella cortex. Compared to those from HC subjects, the PIB showed a marked retention in AD patients in regions such as frontal cortices, temporal and parietal cortices, portions of occipital cortex, and the striatum. However, the uptake and clearance of PIB was almost the same between HC subjects and AD patients in cerebellum and white matter which both lack of fibrillar amyloid plaques. PIB accumulation in cortical areas in AD patients was more significant than that from HC subjects, indicating that increased significant amyloid deposition resulted in increased retention of PIB in these areas in AD. Overall, this study strongly provides new insight that PIB retention may serve as an excellent indicator of amyloid deposits in living subjects. *Figure 2* shows the topographical pattern of PIB retention in both AD patients and HC.

PET imaging of neuroinflammation in AD with ^{11}C-PK11195

Microglial activation may be strongly associated with brain's inflammatory and immune response to neuronal degeneration in AD. Molecular imaging has been capable to investigate the neuroinflammation pathophysiological process in AD. The examination of activated microglia using PET may serve as an *in vivo* marker of CNS disorder activity. The activated microglia will be greatly increased with the expression of the PBR. The 1-(2-chlorophenyl)-N-methyl-N-(1-methylpropyl)-3-isoquinoline carboxamide (PK11195) is a prototype synthetic ligand used specifically for PBR (43,44). Labeled with carbon-11, PK11195 can be used as a PET tracer for the measurement of neuroinflammation. For example, Cagnin *et al*. (43) have employed the ^{11}C *(R)*-PK11195 to explore the microglial activation in the early stages of AD. They studied eight AD patients and 15 healthy subjects using PET combined with MRI. All participants were injected the ^{11}C *(R)*-PK11195 with a mean of 360 MBq. Their results showed that for healthy subjects, the ^{11}C *(R)*-PK11195 binding was lower in all regions except the thalamus if compared to that from the background. Interestingly ^{11}C *(R)*-PK11195 binding also exhibited a significant age-related increase. In contrast, for AD patients, significantly elevated regional ^{11}C *(R)*-PK11195 binding was found in temporoparietal cortex, fusiform gyrus, amygdala, posterior cingulate cortex (see *Figure 3*). ^{18}FDG-PET findings showed that regions with increased amount of ^{11}C *(R)*-PK11195 binding showed decreased cerebral glucose metabolism consumption (see *Figure 4*). This study has provided *in vivo* evidence that the activated microglia was strongly correlated with classical inflammatory diseases and the anti-inflammatory agents, which may be useful in treating AD. Further, the study has demonstrated that *in vivo* measurement of the PBR can help to identify the AD pathogenesis at the early stage.

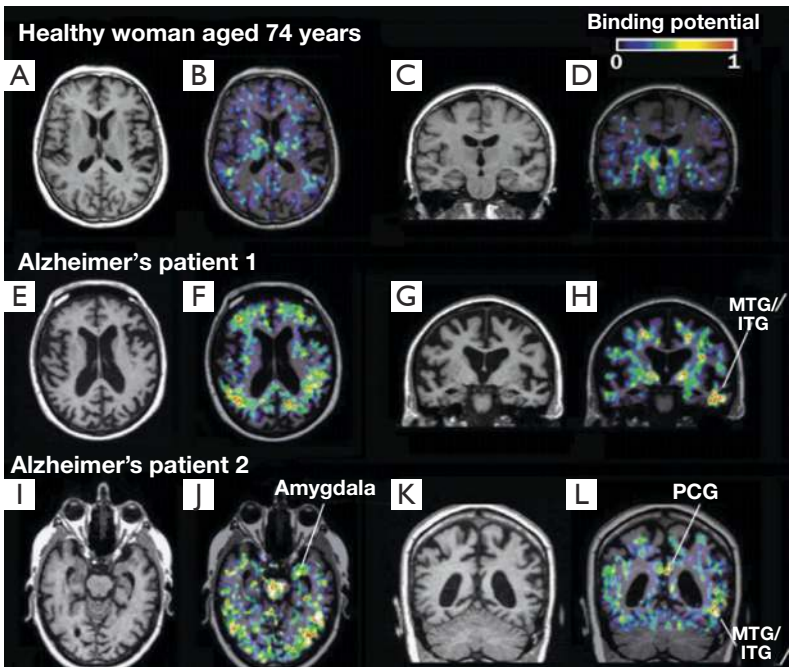

Figure 3 ^{11}C *(R)*-PK11195 binding in HC and AD patients. No significant ^{11}C *(R)*-PK11195 binding in cortex was found in HC [(A,C) T1-weighted MRI images; (B,D) MRI-PET fusion images]; however, in AD with severe dementia (E-H), widespread cortical ^{11}C *(R)*-PK11195 binding was found mainly in the left MTG/ITG; in AD with moderate dementia (I-L), substantial ^{11}C *(R)*-PK11195 binding was found mainly in the left PCG. Reproduced with the permission from ref. (43). HC, healthy controls; AD, Alzheimer's disease; MRI, magnetic resonance imaging; PET, positron emission tomography; MTG, middle temporal gyrus; ITG, inferior temporal gyrus; PCG, posterior cingulate gyrus.

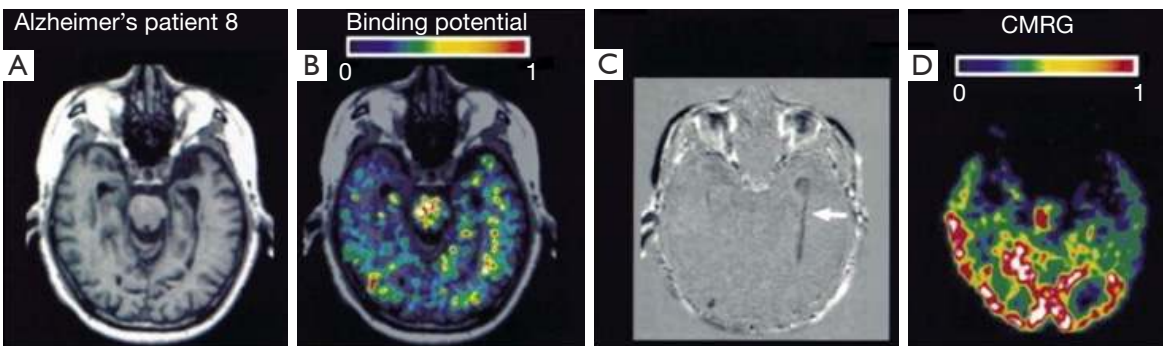

Figure 4 Results of cerebral glucose metabolism with ^{18}FDG-PET. (B) Indicates the PK11195 images co-registered and fused to MRI; (C) stands for subtraction MRI obtained half to one year after the ^{11}C *(R)*-PK11195 PET scan; in AD patient 8, regions such as temporal lobe (B) with high ^{11}C *(R)*-PK11195 binding have subsequently undergone atrophy (C) after half a year. The white arrow shows volume loss of hypointense areas; (D) reveals bilateral hypometabolism done within 1 month of ^{11}C *(R)*-PK11195 PET scan compared with healthy controls, particularly in left temporal lobe. All image volumes have been coregistered into same space. Reproduced with the permission from ref. (43). PET, positron emission tomography; MRI, magnetic resonance imaging; AD, Alzheimer's disease.

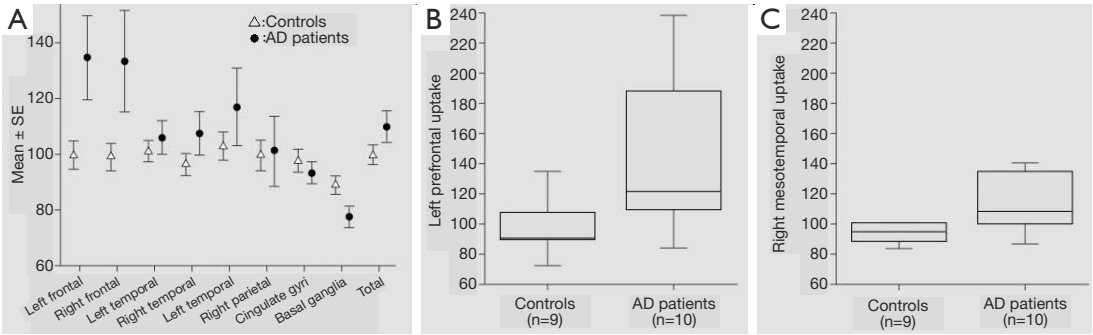

Figure 5 (A) Grouped mean ± standard error of ^{123}I-iodo-PK11195 uptake values; (B) and (C) represents the ^{123}I-iodo-PK11195 uptake values for the left prefrontal and the right mesiotemporal area, respectively. Reproduced with the permission from ref. (24).

SPECT imaging of neuroinflammation in AD with ^{123}I-iodo-PK11195

It should be noted that the application of the above mentioned ^{11}C *(R)*-PK11195 is limited to the PET system and an in-house cyclotron which produced the short half-lived positron-emitting radioisotopes. Previous work has demonstrated that the ^{123}I-iodo-PK11195 is a more appropriate and high-affinity agent for PBR to detect brain lesions by SPECT (45). Recently, Versijpt *et al*. has used ^{123}I-iodo-PK11195 with SPECT to firstly investigate the AD inflammation *in vivo* by measuring the uptake of ^{123}I-iodo-PK11195 when compared with normal individuals (24). Ten AD patients and nine HC were included in their study. Increased mean uptake of ^{123}I-iodo-PK11195 in AD was identified in various areas including frontal, temporal, parietal and occipital areas, indicating that the inflammatory process in AD may spread widely and dispersedly (see *Figure 5*). Overall, though it remains largely unknown whether ^{123}I-iodo-PK11195 SPECT would be strong enough to detect pathological changes at a very early stage of the disease, this study has proved that ^{123}I-iodo-PK11195 could serve as a cellular marker of disease activity to indicate the inflammatory pathology in AD.

PET/SPECT imaging in PD

PD also known as idiopathic Parkinsonism is the second most common progressive neurodegenerative disorder after AD, which characterized by movement-related symptoms including tremor at rest, rigidity, bradykinesia (slowness of movement) and postural instability and also by non-motor symptoms including autonomic dysfunction, neuropsychiatric problems such as cognition impairments, behavior and mood alterations. The disease is pathophysiologically characterized by brain cell death in the pars compacta of the substantia nigra, neuronal loss accompanied with microglia activation and the Lewy bodies. The hallmark of PD pathology is a progressive degeneration of the nigrostriatal dopaminergic neurons (46,47). Molecular imaging like PET and SPECT of the dopaminergic system have been extensively employed to detect the functional and neurochemical changes of PD and other neurodegenerative parkinsonian disorders.

PET studies in PD with ^{11}C-PK11195, ^{11}C-CFT and ^{18}F-dopa

PET studies with ^{11}C-PK11195 for PBR have been used to help measure the activated microglia and better understand the ongoing neurodegenerative process and disease activity in PD patients. Recently, two PET studies have been conducted to measure the microglia activation using ^{11}C-PK11195 and to assess the presynaptic dopamine transporter (DAT) availability using ^{11}C-CFT (48) and ^{18}F-dopa (49). DAT is a membrane protein implicated in the high-affinity uptake of dopamine which can be a potential marker for the integrity of nigrostriatal projections (46). Ouchi *et al*. have examined the levels of ^{11}C-PK11195 and ^{11}C-CFT binding potentials (BPs) in ten early-stage drug-naïve PD patients and ten age-matched normal subjects simultaneously (48). Their studies for the first time showed that the ^{11}C-PK11195 binding in the midbrain was extensively increased in AD patients if compared to that from the healthy subjects. What's more, the midbrain ^{11}C-PK11195 BP in AD was found to be significantly negatively related with ^{11}C-CFT BP in the putamen and positively associated with the motor severity. In contrast, the ^{11}C-PK11195 BP was showed to have an age-dependent increase in the midbrain and thalamus in healthy subjects.

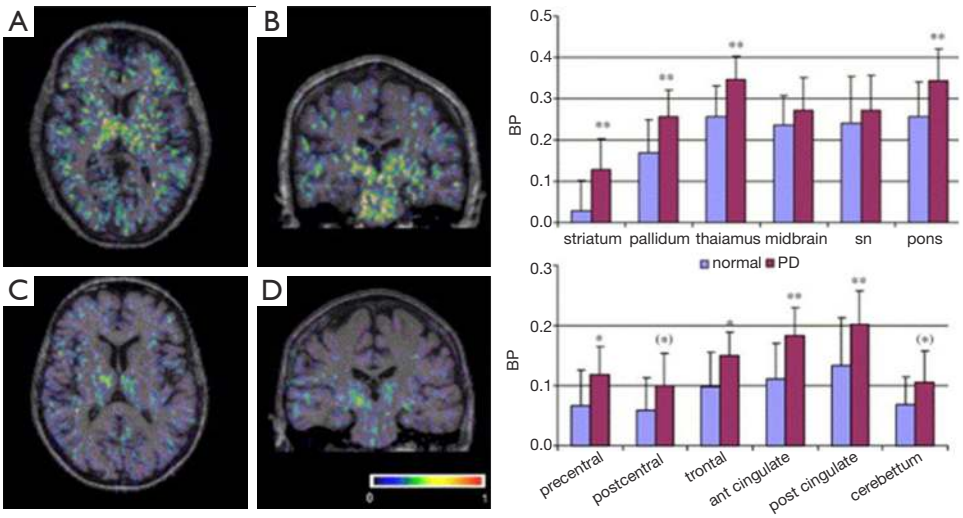

Figure 6 The left figure shows the ^{11}C-PK11195 binding in a Parkinson's disease (PD) patient (A,B) and a healthy control (C,D). The right figure illustrated the mean regional binding potential (BP) values in subcortical and cortical regions in both PD patients and healthy controls. Reproduced with the permission from ref. (49).

Overall, this study supports the idea that the loss of dopaminergic nigrostriatal projection played an important role in the degeneration process in the early stage of PD.

Another study using 18 PD patients and 11 HC using ^{11}C-PK11195 and ^{18}F-dopa PET demonstrated a more widespread microglia activation (49). It is concluded that ^{18}F-dopa PET was the first neuroimaging modality suited for measuring the integrity of presynaptic dopamine (46,50). Gerhard *et al*. (49) have found that the mean ^{11}C-PK11195 BP value in the basal ganglia including the striatum, pallidum and thalamus and the cortex involving precental gyrus, frontal lobe, cingulate gyrus and left hippocampus was higher in PD patients than normal group. Apart from the inverse correlation showed in thalamus and cingulate cortex, there was no significant correlation between the levels of basal ganglia microglial activation and diseased severity or putamen ^{18}F-dopa uptake. In addition, eight PD patients were examined with ^{11}C-PK11195 PET and four of them also underwent with ^{18}F-dopa PET scan after 18-28 months. No significant ^{11}C-PK11195 signal changes occurred during 2 years, suggesting that the microglia are activated early in PD process and then remain stable (49). The ^{11}C-PK11195 binding and the mean regional BP values in a PD patient and a HC are illustrated in *Figure 6*.

SPECT imaging of DAT binding in PD

It should be noted that one of the advantages of the SPECT over PET is its high spatial resolution and the tracers for SPECT are industrial produced and relative long half-live. Brain SPECT imaging of DAT using various radiotracers has become very sensitive to examine the nigrostriatal degeneration of PD and help improve the early diagnosis of the disease since the DAT imaging is abnormal at the early stage of PD (47). The specific SPECT radiotracers for DAT include Iodine-123-β-carbomethoxy-3β-[4-iodophenyltropane] (^{123}I-β-CIT), (Iodine-123-N-[3-fluoropropyl]-2β-carbomethoxy-3β-[4-iodophenyl]) (^{123}I-FP-CIT) and ^{99m}Tc-TRODAT-1.

^{123}I-β-CIT is a cocaine derivative radiotracer which binds with high affinity to dopamine and serotonin transporters with a prolonged time of striatal uptake at 14-24 hours post injection. Many studies have indicated that ^{123}I-β-CIT SPECT enables to quantitatively measure the concentration of striatal DATs, which can be helpful in diagnosis of PD (27). A number of studies have showed a correlation between the decreased striatal ^{123}I-β-CIT binding and the symptom severity in PD (51-54). A prior study has demonstrated that the sensitivity and specificity of ^{123}I-β-CIT SPECT are age-related. Particularly, in younger PD patients with their age less than 55 years, the ^{123}I-β-CIT SPECT are 100% sensitive and specific for the diagnosis (55). In addition, patients with hemiparkinsonism demonstrated greater uptake reduction of ^{123}I-β-CIT in the stratum contralateral side to symptom side as well as ipsilateral side when compared with those from the healthy subjects (53,56,57). ^{123}I-β-CIT SPECT could be of great

value in detecting PD at a very early stage or even the presymptomatic stage. Nonetheless, ^{123}I-β-CIT suffers from a potential disadvantage that it takes a prolonged time of striatal uptake kinetics after its injection. In this regard, the ^{123}I-FP-CIT which is an analogue of ^{123}I-β-CIT could take within hours to maximal striatal uptake following its administration.

^{123}I-FP-CIT has been applied for investigating the dopaminergic nigrostriatal neurons degeneration in the early stage of PD. For example, Spiegel *et al*. reported that both affected and unaffected striatal ^{123}I-FP-CIT binding ratios were associated significantly with the motor score of the Unified PD rating scale. In contrast, FP-CIT distribution showed no significant correlation with age, disease duration or gender of the patients (58). However, another study has found contradicted results that the uptake of FP-CIT in the striatum, caudate and putamen were related with disease duration (59). More recently, Filippi *et al*. have described a bilateral DAT loss in early PD with one-side clinical symptoms and preclinical DAT loss in the ipsilateral striatal binding using semi-quantitative ^{123}I-FP-CIT SPECT, suggesting that semi-quantitative analysis may be helpful to the early diagnosis of PD as well as the bilateral dopaminergic damage (60). What's more, a European multicenter, prospective and longitudinal study with SPECT using ^{123}I-FP-CIT has reported that the mean sensitivity of ^{123}I-FP-CIT SPECT for diagnosis of PD was 78.0% and the mean specificity was 96.8% (61). Over all, SPECT with ^{123}I-labeled DAT ligands might be very useful in the diagnosis of PD in the preclinical and asymptomatic stage. Nonetheless, few ^{123}I-labeled ligands have been widely applied for DAT imaging due to their relatively high cost and limited availability.

In contrast, the relative low-cost and easy obtainable ^{99m}Tc-labeled tracers with an optical energy and half-life could be more widely used for routine DAT imaging (62). There are many ^{99m}Tc-labeled ligands of DAT based on cocaine or tropane derivative (28,63,64). Among those, a ^{99m}Tc-labeled tropane derivative, [2-[[2-[[[3-(4-chlorophenyl)-8-methyl-8-azabicyclo[3,2,1]oct-2-yl]methyl](2-mercaptoethyl) amino]ethyl]amino]ethane-thiolato(3-)-*N2*,*N2*',*S2*,*S2*] oxo-[1R-(exo-exo)](TRODAT-1), which is the first ^{99m}Tc-labeled ligand available for DAT imaging has been found to show advantage and promise in human study. A number of studies have suggested that the ^{99m}Tc-TRODAT-1 is an ideal radiotracer that binds with high affinity to the DATs. Researches have indicated that the ^{99m}Tc-TRODAT-1 SPECT is valuable and feasible to assess the integrity of dopamine neurons for the diagnosis of PD, they found that the TRODAT uptake in the striatum was significantly decreased in PD patients (62,64). A prior study investigated patients with Clinically Unclear Parkinsonian Syndromes (CUPS) using ^{99m}Tc-TRODAT-1 SPECT has found that the sensitivity and the specificity was 100% and 70% respectively, indicating that the TRODAT-1 may be helpful in the diagnosis of even preclinical stage of PD patients (65,66). Another study aimed to evaluate the diagnosis accuracy of ^{99m}Tc-TRODAT-1 SPECT showed a remarkable reduction of mean TRODAT uptake value in the caudate, anterior and posterior putamen in early PD patients compared to normal individuals. Statistical analysis using the mean of ipsilateral and contralateral posterior putamen as region of interest can achieve a maximal sensitivity of 79% and specificity of 92%. The results may shed light on that the TRODAT SPECT imaging can accurately distinguish mild PD patients from healthy subjects, suggesting the TRODAT be a valuable technique to improve the diagnosis of patients with early signs and symptoms of PD (67).

Conclusions

In conclusion, molecular imaging methods have enabled *in vivo* assessment of molecular processes related to the CNS disorders combined with high specific molecular probes. PET and SPECT are useful and reliable tools for clinical molecular neuroimaging. The unique ability of the nuclear molecular imaging to image *in vivo* changes in brain biochemistry such as Aβ deposition, neurotransmitter turnover and metabolism is able to help us better understand the pathology mechanisms underlying CNS diseases. Compared to PET, it is difficult for SPECT to obtain a reliable quantification. Besides, the image resolution of SPECT is also limited for the visualization of basal ganglia. However, SPECT is more practical as a routine procedure than PET. Progress in the sensitivity and spatial resolution and the variety of the molecular probes available for PET and SPECT will help further identify the biomarkers for biochemical processes of CNS diseases. Overall, the PET and SPECT imaging of brain function showed their tremendous promises for improving early diagnosis and treatment of CNS diseases.

Acknowledgements

The study is supported by SRG2013-00035-FHS Grant,

MYRG2014-00093-FHS Grant from University of Macau in Macau and FDCT grant 026/2014/A1 from Macao government.

Disclosure: The authors declare no conflict of interest.

References

1. James ML, Gambhir SS. A molecular imaging primer: modalities, imaging agents, and applications. Physiol Rev 2012;92:897-965.
2. Weissleder R, Mahmood U. Molecular imaging. Radiology 2001;219:316-33.
3. Kim E, Howes OD, Kapur S. Molecular imaging as a guide for the treatment of central nervous system disorders. Dialogues Clin Neurosci 2013;15:315-28.
4. Balas C. Review of biomedical optical imaging—a powerful, non-invasive, non-ionizing technology for improving in vivo diagnosis. Meas Sci Technol 2009;20:104020.
5. Phelps ME. Positron emission tomography provides molecular imaging of biological processes. Proc Natl Acad Sci U S A 2000;97:9226-33.
6. Strijckmans K. The isochronous cyclotron: principles and recent developments. Comput Med Imaging Graph 2001;25:69-78.
7. Halldin C, Gulyás B, Langer O, Farde L. Brain radioligands--state of the art and new trends. Q J Nucl Med 2001;45:139-52.
8. Ido T, Wan C, Carella V, Fowler JS, Wolf AP, Reivich M, Kuhl DE. Labeled 2-deoxy-D-glucose analogs: 18F-labeled 2-deoxy-2-fluoro-D-glucose, 2-deoxy-2-fluoro-D-mannose and 14C-2-deoxy-2-fluoro-D-glucose. J Label Compds Radiopharm 1978;24:174-83.
9. Beekman FJ, van der Have F, Vastenhouw B, van der Linden AJ, van Rijk PP, Burbach JP, Smidt MP. U-SPECT-I: a novel system for submillimeter-resolution tomography with radiolabeled molecules in mice. J Nucl Med 2005;46:1194-200.
10. van der Meel R, Gallagher WM, Oliveira S, O'Connor AE, Schiffelers RM, Byrne AT. Recent advances in molecular imaging biomarkers in cancer: application of bench to bedside technologies. Drug Discov Today 2010;15:102-14.
11. Labbe JP. SPECT/CT emerges from the shadow of PET/CT. Biophotonics Int 2003;10:50-7.
12. Hijnen NM, de Vries A, Nicolay K, Grüll H. Dual-isotope 111In/177Lu SPECT imaging as a tool in molecular imaging tracer design. Contrast Media Mol Imaging 2012;7:214-22.
13. Hapdey S, Soret M, Buvat I. Quantification in simultaneous (99m)Tc/(123)I brain SPECT using generalized spectral factor analysis: a Monte Carlo study. Phys Med Biol 2006;51:6157-71.
14. Shoghi-Jadid K, Small GW, Agdeppa ED, Kepe V, Ercoli LM, Siddarth P, Read S, Satyamurthy N, Petric A, Huang SC, Barrio JR. Localization of neurofibrillary tangles and beta-amyloid plaques in the brains of living patients with Alzheimer disease. Am J Geriatr Psychiatry 2002;10:24-35.
15. Brooks DJ, Ibanez V, Sawle GV, Quinn N, Lees AJ, Mathias CJ, Bannister R, Marsden CD, Frackowiak RS. Differing patterns of striatal 18F-dopa uptake in Parkinson's disease, multiple system atrophy, and progressive supranuclear palsy. Ann Neurol 1990;28:547-55.
16. Mintun MA, Larossa GN, Sheline YI, Dence CS, Lee SY, Mach RH, Klunk WE, Mathis CA, DeKosky ST, Morris JC. [11C]PIB in a nondemented population: potential antecedent marker of Alzheimer disease. Neurology 2006;67:446-52.
17. Klunk WE, Engler H, Nordberg A, Wang Y, Blomqvist G, Holt DP, Bergström M, Savitcheva I, Huang GF, Estrada S, Ausén B, Debnath ML, Barletta J, Price JC, Sandell J, Lopresti BJ, Wall A, Koivisto P, Antoni G, Mathis CA, Långström B. Imaging brain amyloid in Alzheimer's disease with Pittsburgh Compound-B. Ann Neurol 2004;55:306-19.
18. Farde L, Wiesel FA, Stone-Elander S, Halldin C, Nordström AL, Hall H, Sedvall G. D2 dopamine receptors in neuroleptic-naive schizophrenic patients. A positron emission tomography study with [11C]raclopride. Arch Gen Psychiatry 1990;47:213-9.
19. Hirvonen J, Karlsson H, Kajander J, Markkula J, Rasi-Hakala H, Någren K, Salminen JK, Hietala J. Striatal dopamine D2 receptors in medication-naive patients with major depressive disorder as assessed with [11C]raclopride PET. Psychopharmacology (Berl) 2008;197:581-90.
20. Banati RB, Newcombe J, Gunn RN, Cagnin A, Turkheimer F, Heppner F, Price G, Wegner F, Giovannoni G, Miller DH, Perkin GD, Smith T, Hewson AK, Bydder G, Kreutzberg GW, Jones T, Cuzner ML, Myers R. The peripheral benzodiazepine binding site in the brain in multiple sclerosis: quantitative in vivo imaging of microglia as a measure of disease activity. Brain 2000;123:2321-37.
21. Groom GN, Junck L, Foster NL, Frey KA, Kuhl DE. PET of peripheral benzodiazepine binding sites in the microgliosis of Alzheimer's disease. J Nucl Med

1995;36:2207-10.
22. Savic I, Thorell JO, Roland P. [11C]flumazenil positron emission tomography visualizes frontal epileptogenic regions. Epilepsia 1995;36:1225-32.
23. Kadir A, Almkvist O, Wall A, Långström B, Nordberg A. PET imaging of cortical 11C-nicotine binding correlates with the cognitive function of attention in Alzheimer's disease. Psychopharmacology (Berl) 2006;188:509-20.
24. Versijpt JJ, Dumont F, Van Laere KJ, Decoo D, Santens P, Audenaert K, Achten E, Slegers G, Dierckx RA, Korf J. Assessment of neuroinflammation and microglial activation in Alzheimer's disease with radiolabelled PK11195 and single photon emission computed tomography. A pilot study. Eur Neurol 2003;50:39-47.
25. Arlicot N, Katsifis A, Garreau L, Mattner F, Vergote J, Duval S, Kousignian I, Bodard S, Guilloteau D, Chalon S. Evaluation of CLINDE as potent translocator protein (18 kDa) SPECT radiotracer reflecting the degree of neuroinflammation in a rat model of microglial activation. Eur J Nucl Med Mol Imaging 2008;35:2203-11.
26. Booij J, Habraken JB, Bergmans P, Tissingh G, Winogrodzka A, Wolters EC, Janssen AG, Stoof JC, van Royen EA. Imaging of dopamine transporters with iodine-123-FP-CIT SPECT in healthy controls and patients with Parkinson's disease. J Nucl Med 1998;39:1879-84.
27. Winogrodzka A, Bergmans P, Booij J, van Royen EA, Stoof JC, Wolters EC. [(123)I]beta-CIT SPECT is a useful method for monitoring dopaminergic degeneration in early stage Parkinson's disease. J Neurol Neurosurg Psychiatry 2003;74:294-8.
28. Kung HF, Kim HJ, Kung MP, Meegalla SK, Plössl K, Lee HK. Imaging of dopamine transporters in humans with technetium-99m TRODAT-1. Eur J Nucl Med 1996;23:1527-30.
29. Friedland RP, Kalaria R, Berridge M, Miraldi F, Hedera P, Reno J, Lyle L, Marotta CA. Neuroimaging of vessel amyloid in Alzheimer's disease. Ann N Y Acad Sci 1997;826:242-7.
30. Maggio JE, Stimson ER, Ghilardi JR, Allen CJ, Dahl CE, Whitcomb DC, Vigna SR, Vinters HV, Labenski ME, Mantyh PW. Reversible in vitro growth of Alzheimer disease beta-amyloid plaques by deposition of labeled amyloid peptide. Proc Natl Acad Sci U S A 1992;89:5462-6.
31. Friedland RP, Majocha RE, Reno JM, Lyle LR, Marotta CA. Development of an anti-A beta monoclonal antibody for in vivo imaging of amyloid angiopathy in Alzheimer's disease. Mol Neurobiol 1994;9:107-13.
32. Lee HJ, Zhang Y, Zhu C, Duff K, Pardridge WM. Imaging brain amyloid of Alzheimer disease in vivo in transgenic mice with an Abeta peptide radiopharmaceutical. J Cereb Blood Flow Metab 2002;22:223-31.
33. Mathis CA, Wang Y, Holt DP, Huang GF, Debnath ML, Klunk WE. Synthesis and evaluation of 11C-labeled 6-substituted 2-arylbenzothiazoles as amyloid imaging agents. J Med Chem 2003;46:2740-54.
34. Zhuang ZP, Kung MP, Wilson A, Lee CW, Pl?ssl K, Hou C, Holtzman DM, Kung HF. Structure-activity relationship of imidazo[1,2-a]pyridines as ligands for detecting beta-amyloid plaques in the brain. J Med Chem 2003;46:237-43.
35. Wadghiri YZ, Sigurdsson EM, Sadowski M, Elliott JI, Li Y, Scholtzova H, Tang CY, Aguinaldo G, Pappolla M, Duff K, Wisniewski T, Turnbull DH. Detection of Alzheimer's amyloid in transgenic mice using magnetic resonance microimaging. Magn Reson Med 2003;50:293-302.
36. Poduslo JF, Wengenack TM, Curran GL, Wisniewski T, Sigurdsson EM, Macura SI, Borowski BJ, Jack CR Jr. Molecular targeting of Alzheimer's amyloid plaques for contrast-enhanced magnetic resonance imaging. Neurobiol Dis 2002;11:315-29.
37. Maruyama M, Maeda J, Ji B, Zhang MR, Okauchi T, Ono M, Hattori S, Trojanowski JQ, Lee VM, Fukumura T, Higuchi M, Suhara T. In vivo optical and PET detections of fibrillar tau lesions in a mouse model of tauopathies. Alzheimer's & Dementia 2009;5:209-10.
38. Okamura N, Suemoto T, Furumoto S, Suzuki M, Shimadzu H, Akatsu H, Yamamoto T, Fujiwara H, Nemoto M, Maruyama M, Arai H, Yanai K, Sawada T, Kudo Y. Quinoline and benzimidazole derivatives: candidate probes for in vivo imaging of tau pathology in Alzheimer's disease. J Neurosci 2005;25:10857-62.
39. Fodero-Tavoletti MT, Okamura N, Furumoto S, Mulligan RS, Connor AR, McLean CA, Cao D, Rigopoulos A, Cartwright GA, O'Keefe G, Gong S, Adlard PA, Barnham KJ, Rowe CC, Masters CL, Kudo Y, Cappai R, Yanai K, Villemagne VL. 18F-THK523: a novel in vivo tau imaging ligand for Alzheimer's disease. Brain 2011;134:1089-100.
40. Thompson PW, Ye L, Morgenstern JL, Sue L, Beach TG, Judd DJ, Shipley NJ, Libri V, Lockhart A. Interaction of the amyloid imaging tracer FDDNP with hallmark Alzheimer's disease pathologies. J Neurochem 2009;109:623-30.
41. Mathis CA, Bacskai BJ, Kajdasz ST, McLellan ME, Frosch MP, Hyman BT, Holt DP, Wang Y, Huang GF, Debnath ML, Klunk WE. A lipophilic thioflavin-T derivative for

positron emission tomography (PET) imaging of amyloid in brain. Bioorg Med Chem Lett 2002;12:295-8.
42. Bacskai BJ, Hickey GA, Skoch J, Kajdasz ST, Wang Y, Huang GF, Mathis CA, Klunk WE, Hyman BT. Four-dimensional multiphoton imaging of brain entry, amyloid binding, and clearance of an amyloid-beta ligand in transgenic mice. Proc Natl Acad Sci U S A 2003;100:12462-7.
43. Cagnin A, Brooks DJ, Kennedy AM, Gunn RN, Myers R, Turkheimer FE, Jones T, Banati RB. In-vivo measurement of activated microglia in dementia. Lancet 2001;358:461-7.
44. Cagnin A, Kassiou M, Meikle SR, Banati RB. Positron emission tomography imaging of neuroinflammation. Neurotherapeutics 2007;4:443-52.
45. Chalon S, Pellevoisin C, Bodard S, Vilar MP, Besnard JC, Guilloteau D. Iodinated PK 11195 as an ex vivo marker of neuronal injury in the lesioned rat brain. Synapse 1996;24:334-9.
46. Pavese N, Brooks DJ. Imaging neurodegeneration in Parkinson's disease. Biochim Biophys Acta 2009;1792:722-9.
47. Wang L, Zhang Q, Li H, Zhang H. SPECT molecular imaging in Parkinson's disease. J Biomed Biotechnol 2012;2012:412486.
48. Ouchi Y, Yoshikawa E, Sekine Y, Futatsubashi M, Kanno T, Ogusu T, Torizuka T. Microglial activation and dopamine terminal loss in early Parkinson's disease. Ann Neurol 2005;57:168-75.
49. Gerhard A, Pavese N, Hotton G, Turkheimer F, Es M, Hammers A, Eggert K, Oertel W, Banati RB, Brooks DJ. In vivo imaging of microglial activation with [11C](R)-PK11195 PET in idiopathic Parkinson's disease. Neurobiol Dis 2006;21:404-12.
50. Cumming P, Borghammer P. Molecular imaging and the neuropathologies of Parkinson's disease. Curr Top Behav Neurosci 2012;11:117-48.
51. Seibyl JP, Marek KL, Quinlan D, Sheff K, Zoghbi S, Zea-Ponce Y, Baldwin RM, Fussell B, Smith EO, Charney DS, Hoffer PB, Innis RB. Decreased single-photon emission computed tomographic [123I]beta-CIT striatal uptake correlates with symptom severity in Parkinson's disease. Ann Neurol 1995;38:589-98.
52. Müller T, Farahati J, Kuhn W, Eising EG, Przuntek H, Reiners C, Coenen HH. [123I]beta-CIT SPECT visualizes dopamine transporter loss in de novo parkinsonian patients. Eur Neurol 1998;39:44-8.
53. Haapaniemi TH, Ahonen A, Torniainen P, Sotaniemi KA, Myllylä VV. [123I]beta-CIT SPECT demonstrates decreased brain dopamine and serotonin transporter levels in untreated parkinsonian patients. Mov Disord 2001;16:124-30.
54. Asenbaum S, Brücke T, Pirker W, Podreka I, Angelberger P, Wenger S, Wöber C, Müller C, Deecke L. Imaging of dopamine transporters with iodine-123-beta-CIT and SPECT in Parkinson's disease. J Nucl Med 1997;38:1-6.
55. Eerola J, Tienari PJ, Kaakkola S, Nikkinen P, Launes J. How useful is [123I]beta-CIT SPECT in clinical practice? J Neurol Neurosurg Psychiatry 2005;76:1211-6.
56. Marek KL, Seibyl JP, Zoghbi SS, Zea-Ponce Y, Baldwin RM, Fussell B, Charney DS, van Dyck C, Hoffer PB, Innis RP. [123I] beta-CIT/SPECT imaging demonstrates bilateral loss of dopamine transporters in hemi-Parkinson's disease. Neurology 1996;46:231-7.
57. Brücke T, Asenbaum S, Pirker W, Djamshidian S, Wenger S, Wöber Ch, Müller Ch, Podreka I. Measurement of the dopaminergic degeneration in Parkinson's disease with [123I]β-CIT and SPECT. In: Riederer P, Calne DB, Horowski R, Mizuno Y, Poewe W, Youdim MB. eds. Advances in Research on Neurodegeneration. Vienna: Springer Vienna, 1997:9-24.
58. Spiegel J, Möllers MO, Jost WH, Fuss G, Samnick S, Dillmann U, Becker G, Kirsch CM. FP-CIT and MIBG scintigraphy in early Parkinson's disease. Mov Disord 2005;20:552-61.
59. Benamer HT, Patterson J, Wyper DJ, Hadley DM, Macphee GJ, Grosset DG. Correlation of Parkinson's disease severity and duration with 123I-FP-CIT SPECT striatal uptake. Mov Disord 2000;15:692-8.
60. Filippi L, Manni C, Pierantozzi M, Brusa L, Danieli R, Stanzione P, Schillaci O. 123I-FP-CIT semi-quantitative SPECT detects preclinical bilateral dopaminergic deficit in early Parkinson's disease with unilateral symptoms. Nucl Med Commun 2005;26:421-6.
61. Marshall VL, Reininger CB, Marquardt M, Patterson J, Hadley DM, Oertel WH, Benamer HT, Kemp P, Burn D, Tolosa E, Kulisevsky J, Cunha L, Costa D, Booij J, Tatsch K, Chaudhuri KR, Ulm G, Pogarell O, Höffken H, Gerstner A, Grosset DG. Parkinson's disease is overdiagnosed clinically at baseline in diagnostically uncertain cases: a 3-year European multicenter study with repeat [123I]FP-CIT SPECT. Mov Disord 2009;24:500-8.
62. Mozley PD, Schneider JS, Acton PD, Plössl K, Stern MB, Siderowf A, Leopold NA, Li PY, Alavi A, Kung HF. Binding of [99mTc]TRODAT-1 to dopamine transporters in patients with Parkinson's disease and in healthy

volunteers. J Nucl Med 2000;41:584-9.
63. Meltzer PC, Blundell P, Jones AG, Mahmood A, Garada B, Zimmerman RE, Davison A, Holman BL, Madras BK. A technetium-99m SPECT imaging agent which targets the dopamine transporter in primate brain. J Med Chem 1997;40:1835-44.
64. Huang WS, Lin SZ, Lin JC, Wey SP, Ting G, Liu RS. Evaluation of early-stage Parkinson's disease with 99mTc-TRODAT-1 imaging. J Nucl Med 2001;42:1303-8.
65. Sawada H, Oeda T, Yamamoto K, Kitagawa N, Mizuta E, Hosokawa R, Ohba M, Nishio R, Yamakawa K, Takeuchi H, Shimohama S, Takahashi R, Kawamura T. Diagnostic accuracy of cardiac metaiodobenzylguanidine scintigraphy in Parkinson disease. Eur J Neurol 2009;16:174-82.
66. Leite MA, Nascimento OJ. Diagnostic accuracy of cardiac metaiodobenzylguanidine scintigraphy in Parkinson disease. Eur J Neurol 2010;17:e9; author reply e10.
67. Chou KL, Hurtig HI, Stern MB, Colcher A, Ravina B, Newberg A, Mozley PD, Siderowf A. Diagnostic accuracy of [99mTc]TRODAT-1 SPECT imaging in early Parkinson's disease. Parkinsonism Relat Disord 2004;10:375-9.

Cite this article as: Lu FM, Yuan Z. PET/SPECT molecular imaging in clinical neuroscience: recent advances in the investigation of CNS diseases. Quant Imaging Med Surg 2015;5(3):433-447. doi: 10.3978/j.issn.2223-4292.2015.03.16

